FLUCOME 2009
10th International Conference on Fluid Control, Measurements, and Visualization
August 17–21, 2009, Moscow, Russia

THREE-DIMENSIONAL FLOW VISUALIZATION AND PIV MEASUREMENT IN NEAR FIELD OF STRONGLY BUOYANT JET

Nobuyuki Fujisawa[1], Tomoaki Syuto[2], Tsuyushi Takasugi[3] and Takayuki Yamagata[4]

ABSTRACT

The near-field structure of strongly buoyant jet issuing from a square nozzle at low Froude and Reynolds numbers is studied by using three-dimensional LIF flow visualization and scanning PIV. These experimental techniques allow the visualization of unsteady three-dimensional flow phenomenon occurring in the near-field of strongly buoyant jet. It is found that the buoyant jet is unstable to the positive buoyancy forces, which promote the inflow motion near the nozzle exit. The surrounding low temperature fluid moves into the nozzle along the nozzle corner and mixes with the high temperature fluid deep into the nozzle. Then, the flow pattern inside the nozzle becomes highly complex to promote the laminar to turbulent transition of the vertical buoyant jet. The statistical flow characteristics of the strongly buoyant jet are evaluated from the three-dimensional scanning PIV measurement, and the result indicates the presence of axisymmetric mean-flow and velocity fluctuations along the interface between the main flow and the inflow in the nozzle.

Keywords: flow visualization, three-dimensional flow, buoyant jet, LIF, PIV, turbulence

INTRODUCTION

The buoyant flows are of great importance in many engineering problems related to fluid and thermal sciences. Examples of buoyant flows are observed in some atmospheric environments, such as spreading of smoke from chimney and drain, and in industrial flow-problems of pollution. The buoyant jet is termed by the buoyancy dominated flow issuing from a nozzle with a certain magnitude of momentum flux. Therefore, the fluid motion of buoyant jet is governed by inertial, buoyant and viscous forces, which are often characterized by Froude and Reynolds numbers.

The classical works on buoyant jet are mostly concerned with the experimental studies on mean flow characteristics of the jets. The preliminary results on this subject are summarized by Chen and Rodi (1980) and List (1982), but most of them are concerned with the mean flow characteristics of fully developed region. Among these basic studies, some special attentions are placed on the stability and the laminar to turbulent transition of the buoyant jets by Anwar (1972), Mollendorf and Gebhart(1973), Ungate et al. (1975) and Pasumarthi and Agrawal (2005). It is found that the laminar buoyant jet is

[1] Corresponding author: Visualization Research Center, Niigata University, Japan, e-mail: fujisawa@eng.niigata-u.ac.jp
[2] Visualization Research Center, Niigata University, Japan
[3] Visualization Research Center, Niigata University, Japan
[4] Visualization Research Center, Niigata University, Japan

destabilized by the growth of asymmetric disturbances. The laminar length of the jet is decreased by the influence of positive buoyancy, and it increases with a decrease in Reynolds numbers (Mollendorf and Gebhart 1973, Subbarao and Cantwell 1992). Later, turbulence measurements in the buoyant jets are reported by Papanicolaou and List (1988), Murota et al. (1989), Shabbir and George (1994), Dai et al. (1994), who measured the turbulence characteristics of velocities and temperatures, using point measurement techniques, such as laser Doppler velocimetry, hot wire/film, thermocouple and laser-induced fluorescence techniques.

More recently, the structure of buoyant jet is investigated by Tian and Roberts (2003) and Fujisawa et al.(2008) using PIV and LIF measurements, and by Zhou et al.(2001) and Zhao(2004) using large-eddy simulation. These results indicate that the structure of velocity and temperature field of the buoyant jet is dominated by asymmetrical modes of turbulence, which agrees with the result from the stability analysis by Mollendorf and Gebhart (1973). However, most of the previous studies are focused on the fully developed buoyant jet, so that there is very few knowledge about the near-field structure of buoyant jets. Concerning this topic, Funatani and Fujisawa (2005) conducted the simultaneous measurements of temperature and velocity field of the strongly buoyant jet, using the laser-induced fluorescence technique combined with particle image velocimetry. They found the existence of local peaks of turbulent heat fluxes near the nozzle exit. The appearance of such local peaks may be due to the phenomenon at low Froude and Reynolds numbers in comparison with previous studies of buoyant jets at high Froude and Reynolds numbers. This experimental finding triggers further study of the flow behavior in the near-field of the strongly buoyant jet, which is characterized by low Froude and Reynolds numbers.

The purpose of this paper is to study the near-field flow characteristics of strongly buoyant jet at low Froude and Reynolds numbers issuing from a square nozzle, using three-dimensional flow visualization with laser-induced fluorescence and velocity measurement by scanning PIV to characterize the flow phenomena in the near field. A special attention is placed on the convective motion of the flow inside the nozzle.

EXPERIMENTAL METHODS

Experimental apparatus

The three-dimensional flow visualization and velocity measurement of strongly buoyant jet are carried out using an experimental apparatus as shown in Fig.1. The volume of the test tank is 400 × 400 × 400 mm^3, which is filled with cold water of temperature 10 ℃. The hot water is supplied into the test tank through the bottom square hole having d = 20 mm in side length. A large volume of hot water is prepared in a separate tank with temperature controller, and is supplied to the test tank through the long straight square pipe of 470 mm in length, which is connected to the bottom hole of the test tank. Note that the straight pipe is insulated by Styrofoam. The buoyant jet is generated from the bottom hole of the test tank and is diffused into the stagnant cold-water environment. The temperature of hot water is measured by a thermocouple placed in the settling chamber, which is placed just upstream of the straight pipe, while the bulk velocity of the buoyant jet is controlled by a valve and measured by a flow meter. In the present experiment, the main experiments are carried out at hot water temperature 20℃ and at cold water temperature 10℃, and the bulk velocity through the pipe is kept at 10 mm/s. Therefore, the source Froude number is Fr_0 (= $V_0 / \sqrt{dg(\rho_c - \rho_h)/\rho_h}$) = 0.58 and the Reynolds number is Re (= $V_0 d / \nu$) = 200, where V_0: mean velocity at nozzle exit, g: gravitational acceleration, ν: kinematic viscosity of hot water, ρ: density of fluid, and subscripts c and h denote cold and hot state, respectively.

Flow visualization

The flow visualization is carried out using the fluorescent dye solution (Rhodamine B) illuminated by a CW Nd:YAG laser of 5 W. The light sheet is traversed quickly using a scanner system, which

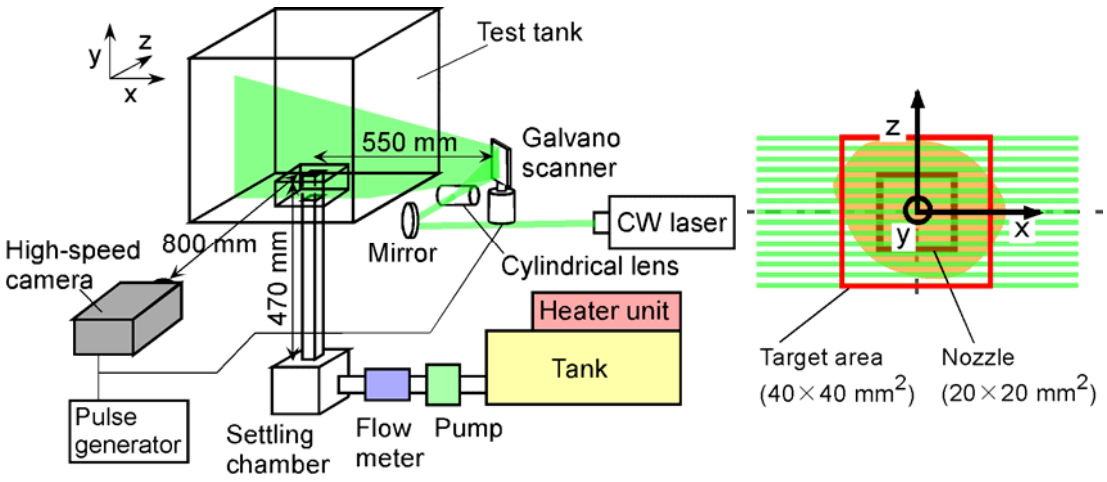

(a) Experimental apparatus **(b) Top view around nozzle exit**

Fig. 1. Experimental apparatus for flow visualization and PIV measurement

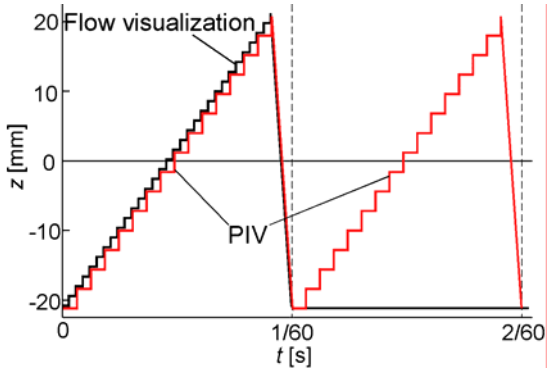

Fig. 2. Time chart of scanning light-sheet

consists of Galvano scanner, mirror and controller as described in Fig.1. This scanner system is located at 550 mm apart from the target flow to provide planar light sheets at various z positions almost parallel to each other. The time chart of scanner system is illustrated in Fig. 2. According to this time chart, the planar light sheet is traversed 40mm in z direction for the first 1/60 s at the velocity of 2.7m/s. After reaching the end of the scanning distance, the light sheet moves back quickly to the original position within 3 ms to repeat the same scanning motion periodically. The synchronous observation is made by a high speed CCD camera operated at 2000 frames/s with a spatial resolution of 1280 × 1024 pixels with 8 bits in gray level. Note that the CCD camera and the scanning system are synchronized by the pulse signal from pulse controller.

Three-dimensional scanning PIV

The periodic illumination and observation using the scanning system in combination with the high speed CCD camera allows the PIV measurement of three-dimensional velocity field of strongly buoyant jet. For this purpose, the flow field is visualized by nylon tracer particles of 80 μm in diameter. The PIV

analysis can be applied to the two images obtained at the first and second scan of the light sheet at the same z position, where the time interval is 1/60 sec (Fig. 2). Then, the planar velocity field at each cross-sections of the buoyant jet can be evaluated. When the time scale of the target flow is much larger than the scanning time period, the three-dimensional velocity field can be almost frozen (Hori and Sakakibara 2004, Fujisawa et al. 2005). This is the case of the present strongly buoyant jet at low Froude and Reynolds numbers. It should be mentioned that the frame rate of the CCD camera is set to 1000 frames/s in the present scanning PIV. This is due to the lower scattering light from the tracer particles than that from the LIF visualization study. It should be mentioned that the planar target area is 40 mm (x) × 90 mm (y) and the scanning distance is 40 mm (z). The particle images are analyzed by cross-correlation algorithm with sub-pixel analysis. The interrogation window size is set to 31 × 31 pixels and the search window size is 41 × 41 pixels. The tracer particles are observed as about 2 pixels and the maximum particle displacement is about 10 pixels, which allows the appearance of error vectors less than 1% of the total number of analyzed velocity vectors. The accuracy of velocity measurement is estimated as 3% with uncertainty interval of 95%.

RESULTS AND DISCUSSIONS

Flow visualization of buoyant jet

In order to examine the near field of buoyant jet, the flow visualization study is carried out using the fluorescence dye of Rhodamine B (Watanabe et al. 2005). Figure 3 shows examples of flow visualization pictures taken at some temperature differences ΔT between the flow and the surrounding fluid, where the mean flow velocity through the nozzle is kept at constant V_0 = 10 mm/s. The flow observations are made by a color CCD camera at the central planar section (x-y plane) of the square nozzle. The flow visualization picture for non-buoyant jet (Fig. 3(a)) indicates the development of the laminar jet upward without any roll-up motion. When the temperature difference ΔT increases to 5℃, the jet flow is accelerated by the buoyancy force and the flow becomes unstable near the nozzle exit, which results in a roll-up motion as shown in Fig. 3(b). Note that the inflow motion is observed near the right hand corner of the square nozzle. With further increase in temperature difference to ΔT = 10 ℃ (Fig. 3(c)) and 30 ℃ (Fig.3(d)), the flow becomes more unstable and the roll-up motion is promoted to appear in a shorter distance from the nozzle exit. Although the jet flow behaves turbulent in the far region of the nozzle, there exists laminar region in and outside the nozzle exit. Therefore, such flow state is considered as unsteady.

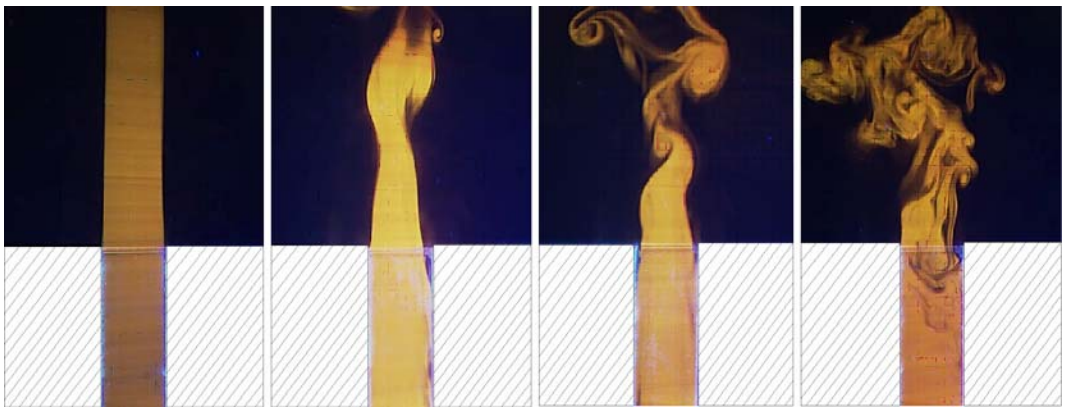

(a) ΔT = 0℃ (b) ΔT =5℃ (c) ΔT = 10℃ (d) ΔT = 30℃

Fig. 3. Examples of LIF flow visualization of buoyant jet (V_0 = 10 mm/s)

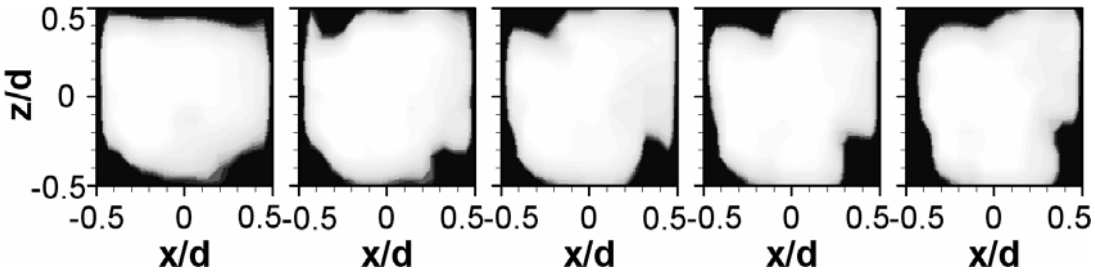

(a) t = 0 s (b) t = 1 s (c) t = 2 s (d) t = 3 s (e) t = 4 s

Fig. 4. LIF flow visualization of buoyant jet in horizontal plane at nozzle exit (Fr_0 = 0.58, Re = 200).

It should be mentioned that unsteady nature of the flow is caused by the buoyancy-induced flow near the nozzle exit. Note that the LIF flow visualization at ΔT =10 ℃ (Fig. 3(c)) corresponds to the flow condition Fr_0 = 0.58, Re = 200, where the three-dimensional visualization is carried out in the present study.

In order to understand the three-dimensional flow behavior of the vertical buoyant jet, the three-dimensional flow visualization study is carried out using the scanning system combined with a high speed camera at Fr_0 = 0.58, Re = 200. Figure 4 shows the time variation of the horizontal cross-sections of LIF visualization at the nozzle exit (y/d = 0). These images are reconstructed from 30 slices of vertical planar images of flow visualization at every 1 sec. These flow visualization results indicate that the dark (low temperature fluid) and bright (high temperature fluid) area moves slowly in the flow field and the fluid motion is found to be unsteady. It can be seen that the low temperature inflow is often observed near the corner of the square nozzle, and the vertical buoyant jet is found near the nozzle center, though the jet contours vary unsteadily.

Instantaneous velocity field of buoyant jet

The three-dimensional scanning PIV measurement of strongly buoyant jet is carried out to understand the variations of three-dimensional velocity characteristics in the near field. Figures 5 and 6 show the instantaneous velocity vectors and the vertical velocities v/V_0 of the buoyant jet reconstructed from the scanning PIV measurement at Fr_0 = 0.58, Re = 200. Figure 5 is the velocity contours at some vertical cross-sections of the buoyant jet. The results indicate that the vertical velocity becomes large even outside the nozzle exit, which is due to the acceleration of the jet velocity by buoyancy forces. It should be mentioned that the inflow velocity appears near the corner of the square nozzle, and it penetrates into the nozzle as deep as 2 to 3 times of the nozzle side length. The inflow velocity distribution is found to be asymmetrical near the nozzle, which corresponds to the swaying growth of the buoyant jet in vertical direction along the nozzle surface. The deflection of the buoyant jet seems to be large as it approaches the nozzle exit. Figure 6 shows the corresponding instantaneous velocity field at some horizontal planes. These results confirm that the inflow velocity is found along the corner of the square nozzle, and the jet flow develops along the nozzle deflecting in side direction. It is also found that the maximum velocity of the buoyant jet shows high peaks even in the outside of the nozzle, and the jet width spreads in horizontal direction.

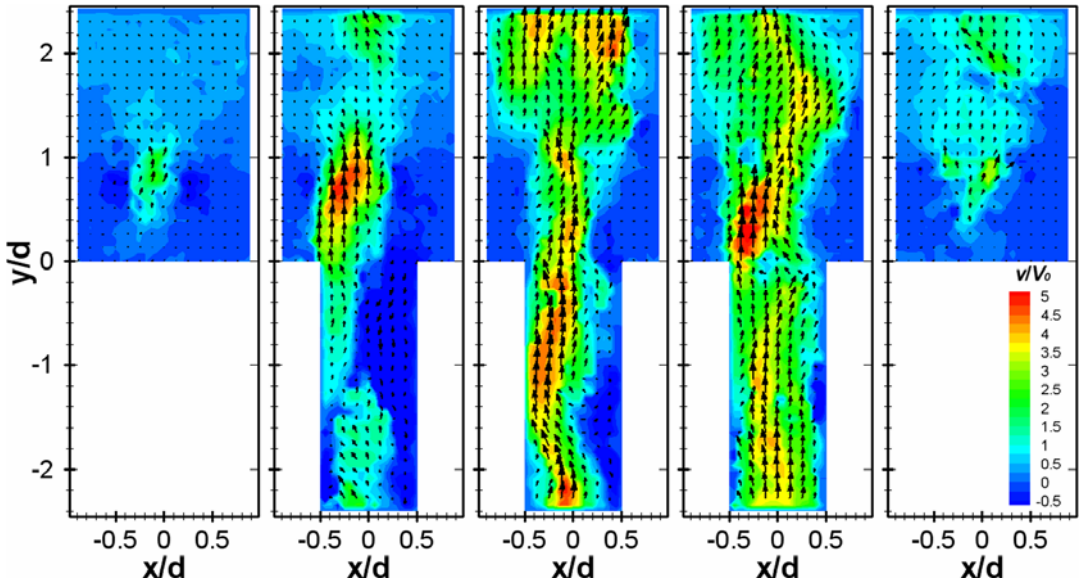

(a) z/d = -0.6 (b) z/d = -0.3 (c) z/d = 0 (d) z/d = 0.3 (e) z/d = 0.6

Fig. 5. Instantaneous velocities of buoyant jet in vertical plane (Fr_0 = 0.58, Re = 200)

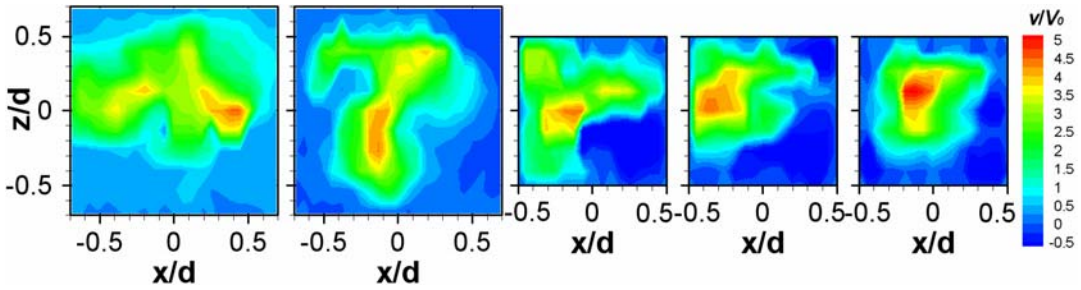

(a) y/d = 2 (b) y/d = 1 (c) y/d = 0 (d) y/d = -1 (e) y/d = -2

Fig. 6. Instantaneous velocities of buoyant jet in horizontal plane (Fr_0 = 0.58, Re = 200)

Mean flow and fluctuating velocity characteristics

The three-dimensional mean velocity field of the buoyant jet is evaluated from 1000 sets of instantaneous velocity fields obtained from the scanning PIV measurement. The results are shown in Figs.7 and 8, which corresponds to the vertical and horizontal slices of the three-dimensional velocity field, respectively. Each figure shows the mean velocity vectors and vertical mean velocities V/V_0. These results indicate that the high temperature fluid moves along the nozzle surface upward and it grows in width as the vertical distance increases, as was expected from the instantaneous velocity fields. The inflow velocity is found near the corner of the square nozzle and it reaches up to 40% of the mean velocity V_0 of the buoyant jet. As the horizontal velocity contour in Fig. 8 is almost circular independent of the vertical distance, the mean velocity field is considered almost axisymmetric about the jet axis. Thus, the mean inflow velocity occurs at four corners of the square nozzle, while the jet flow develops along the nozzle upward by attaching the side surface of the nozzle.

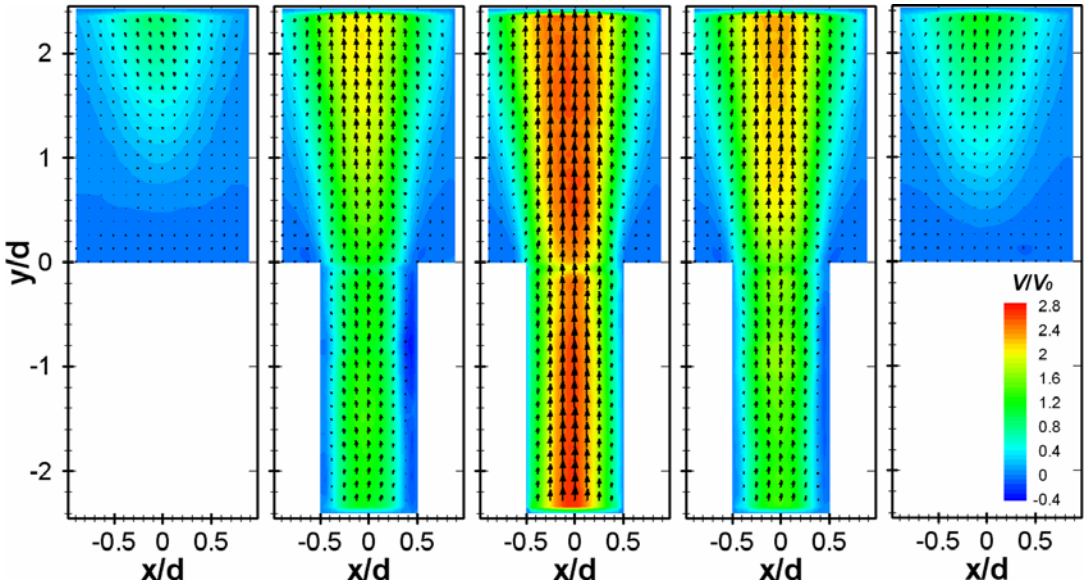

(a) z/d = -0.6 (b) z/d = -0.3 (c) z/d = 0 (d) z/d = 0.3 (e) z/d = 0.6

Fig. 7. Mean velocities of buoyant jet in vertical plane (Fr_0 = 0.58, Re = 200)

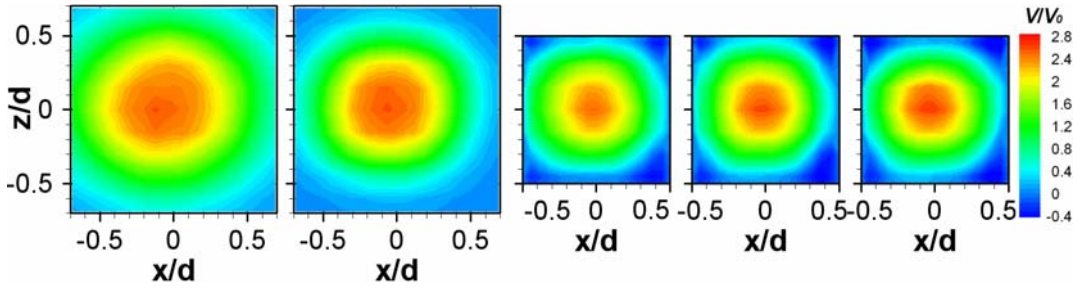

(a) y/d = 2 (b) y/d = 1 (c) y/d = 0 (d) y/d = -1 (e) y/d = -2

Fig. 8. Mean velocities of buoyant jet in horizontal plane (Fr_0 = 0.58, Re = 200)

The velocity fluctuations of the buoyant jet are shown in Figs. 9 and 10, which correspond to the vertical and horizontal slices of the three-dimensional velocity fluctuation field, respectively. These results indicate that large velocity fluctuations are found outside the nozzle exit, but they are still observed in the nozzle, too. The presence of large velocity fluctuations in the nozzle is expected to be due to the unsteady nature of the buoyant jet induced by the inflow motion of the surrounding cold fluid into the nozzle. They are distributed almost in a square shape along the inner surface of the nozzle, which suggests the presence of highly turbulent region in the inflow area along the nozzle corner.

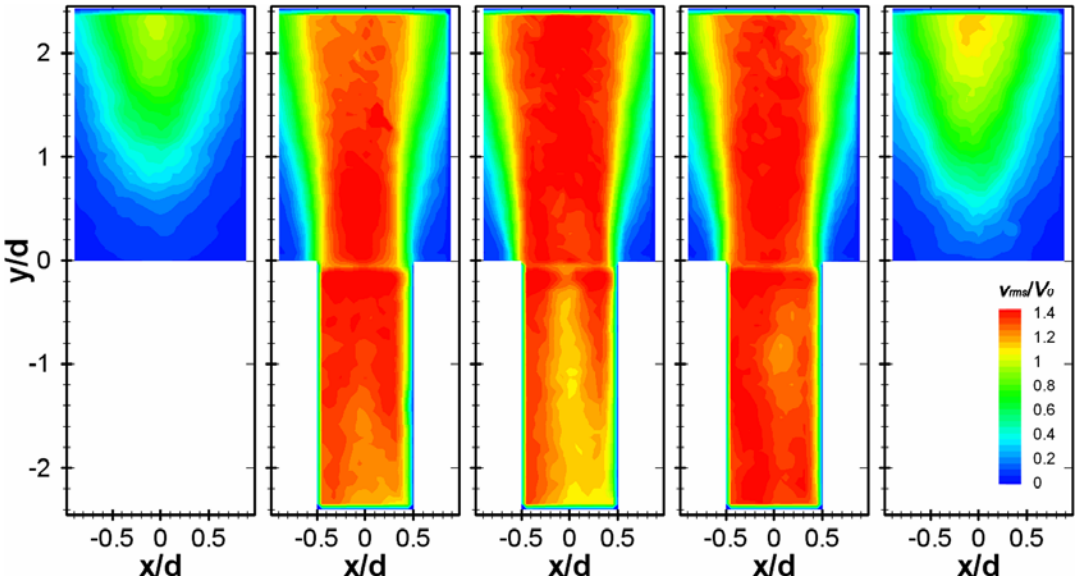

(a) z/d = -0.6 (b) z/d = -0.3 (c) z/d = 0 (d) z/d = 0.3 (e) z/d = 0.6

Fig. 9. Fluctuating velocities of buoyant jet in vertical plane (Fr_0 = 0.58, Re = 200)

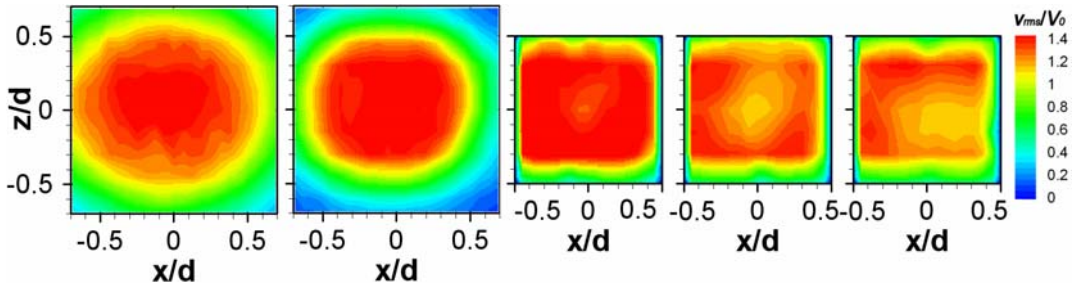

(a) y/d = 2 (b) y/d = 1 (c) y/d = 0 (d) y/d = -1 (e) y/d = -2

Fig. 10. Fluctuating velocities of buoyant jet in horizontal plane (Fr_0 = 0.58, Re = 200)

CONCLUSIONS

The flow characteristics and the structure in the near-field of strongly buoyant jet at low Froude and Reynolds numbers are studied by three-dimensional LIF flow visualization and scanning PIV. The flow visualization study indicates the occurrence of unstable motion near the nozzle exit, which is due to the thermal instability of the buoyant jet at the interface of the hot and surrounding cold fluid. The instantaneous velocity contour measured by scanning PIV shows the presence of unsteady inflow motion near the corner of the square nozzle and the surrounding cold fluid penetrates into the nozzle as deep as 2-3 times of the nozzle side length, which can promote the laminar turbulent transition of the buoyant jet. The mean velocity contour in the horizontal plane shows circular shape, which indicates axisymmetric nature of the mean velocity field. On the other hand, the fluctuating velocity contour in the horizontal plane shows square shape inside the nozzle, indicating the presence of large velocity fluctuations in the inflow area.

REFERENCES

Anwar, H.O. (1972), "Appearance of Unstable Buoyant Jet," J.Hydraulics Division, **HY7,** 1143-1156.

Chen, C.J and Rodi, W. (1980), Vertical Turbulent Buoyant Jets: A Review of Experimental Data, Pergamon, Oxford, UK.

Dai, Z., Tseng, L.-K. and Faeth, G.M. (1994), " Structure of Round, Fully Developed, Buoyant Turbulent Pplumes," J. Heat Transfer, **116**, 409-417.

Fujisawa, N., Funatani, S. and Katoh, N. (2005), "Scanning Liquid-crystal Thermometry and Stereo Velocimetry for Simultaneous Three-dimensional Measurement of Temperature and Velocity Field in a Turbulent Rayleigh-Bernard Convection," Exp. Fluids., **38**, 291-303.

Fujisawa, N., Funatani, S., Watanabe, Y. (2008), "Simultaneous Imaging Techniques for Temperature and Velocity Fields in Thermal Fluid Flows," J. Visualization, **11**, 247-255.

Funatani, S., Fujisawa, N. and Ikeda, H. (2004), " Simultaneous Measurement of Temperature and Velocity Using Two-colour LIF Combined with PIV with a Colour CCD Camera and Its Application to the Turbulent Buoyant Plume," Meas. Sci. Technol., **15**, 983-990.

George, W.K., Alpert, R.L. and Tamanini, F. (1977), "Turbulence Measurements in an Axisymmetric Buoyant Plume," Int. J. Heat Mass Transfer, **20**, 1145-1154.

Hori, T. and Sakakibara, J. (2004), " High-speed Scanning Stereoscopic PIV for 3D Vorticity Measurement in Liquids," Meas. Sci. Technol., **15**, 1067-1078.

List, E.J. (1982), "Turbulent Jets and Plumes," Ann. Rev. Fluid. Mech., **14**, 189-212.

Mollendorf, J.C., Gebhart, B. (1973), "An Experimental and Numerical Study of the Viscous Stability of a Round Laminar Vertical Jet with and without Thermal Buoyancy for Symmetric and Asymmetric Disturbances," J. Fluid Mech., **61,** 367-399.

Murota, A., Nakatsuji, K., Tamai, M. (1989), "Experimental Study on Turbulence Structure in Turbulent Plane Forced Plume," J. Japan Soc. Civ. Eng., **405,** 79-87.

Papanicolaou, P.N., List, E.J. (1988), "Investigations of Round Vertical Turbulent Buoyant Jets," J. Fluid Mech., **195**, 341-391.

Pasumarthi, K.S. and Agrawal, A.K. (2005), "Buoyancy Effects on Flow Transition in Low-density Inertial Gas Jets," Exp. Fluids, **38**, 541-544.

Shabbir, A. and George, W.K. (1994), "Experiments on a Round Turbulent Buoyant Plume," J. Fluid Mech., **275**, 1-32.

Subbarao, E.R., Cantwell, B.J. (1992), "Investigation of Co-flowing Buoyant Jet: Experiments on the Effects of Reynolds Number and Richardson Number," J. Fluid Mech., **245**, 69-90.

Tian, X., Roberts, P.J.W. (2003), "A 3D LIF System for Turbulent Buoyant Jet Flows," Exp. Fluids, **35**, 636-647.

Ungate, C.D., Harleman, D.R.F., Jirka, G.B. (1975), "Stability and Mixing of Submerged Turbulent Jets at Low Reynolds Numbers," Energy Laboratory Report MIT-EL **75-014**.

Watanabe, Y., Hashizume, Y., Fujisawa, N. (2005), "Simultaneous Flow Visualization and PIV Measurement of Turbulent Buoyant Plume," J. Visualization, **8**, 293-294.

Zhou, X., Luo, K.H., Williams, J.J.R. (2001), "Large Eddy Simulation of a Turbulent Forced Plume," Eur. J. Mech. B/Fluids, **20**, 233-254.

Zhou, X., Hitt, D.L. (2004), "Proper Orthogonal Decomposition Analysis of Coherent Structures in a Transient Buoyant Jet," J Turbulence, **5**, 1-21.